Progress In Electromagnetics Research, Vol. 170, 169–176, 2021

Directional Polaritonic Excitation of Circular, Huygens and Janus Dipoles in Graphene-Hexagonal Boron Nitride Heterostructures

Yuyu Jiang[1, 2, 3], Xiao Lin[1, 2, 3, *], and Hongsheng Chen[1, 2, 3, *]

Abstract—Polariton assisted tunable directionality provides an intrinsic ingredient to various micro/nano integrated optical systems. Their capabilities of light manipulation in mesoscopic structures allow numerous beneficial properties in information processing. The realization of active near-field directionality by tuning the input signal of system bias is more preferable than that by reconfiguring the nanostructures. Recent progresses on the multiple hybrid dipole radiations ensure another methodology in realizing tunable directionality. Here we investigate some exotic near-field phenomena in a 5-layer waveguide consisted of graphene and hexagonal boron nitride (hBN) illuminated by hybrid dipole sources such as a Circular dipole, a Huygens dipole or a Janus dipole. We demonstrate divergent behaviors of hybrid polariton excitations subject to various source types and the tunability of switching between phonon-like polaritons and plasmon-like polaritons. We also show that the flipping of the group velocity of excited hybrid polaritons can be used to flexibly tune the transportation direction away from the dipolar sources. To be specific, when the group velocity of supported polariton flips its sign, the energy flow will shift to the opposite side accordingly. Such phenomena are promising in the design of reconfigurable and multifunctional nanophotonic devices.

1. INTRODUCTION

Recent progresses of directional excitations in nanophotonic devices have captured lots of interests. The manipulated energy flow provides various capabilities in information processing with mesoscopic structures [1–5], especially in reconfigurable nanodevices [6], nanoimaging [7], and optical quantum systems [8]. Pioneering works on the directional excitations mostly follow the principle of secondary source radiation superpositions from asymmetric structures [9, 10], as well as an alternative design methodology engineers the light source [11, 12]. Fundamental physics behind those designs is the same: to obtain the constructive interference on one side with the destructive interference on the other side. Such philosophy plays a great role in the highly integrated modern photonic systems. Moreover, advanced fabrication techniques significantly reduce the operational feature size in on-chip photonic systems, which enables the plasmon and phonon polaritons assisted high performance optical processing units [13–15]. Simultaneously, the growing integration scale results in a tiny device that mechanical systems find themselves difficult to integrate [16]. Under this constraint, the asymmetric subwavelength structures become immovable and limit the system tunability. Furthermore, due to material dissipations introduced by subwavelength structures and the phase mismatch between light source and the guiding waveguide, the lifetime of polaritons is quite short [17, 18]. To avoid the loss

Received 1 May 2021, Accepted 11 May 2021, Scheduled 13 May 2021

* Corresponding authors: Hongsheng Chen (hansomchen@zju.edu.cn), Xiao Lin (xiaolinzju@zju.edu.cn).

[1] Interdisciplinary Center for Quantum Information, State Key Laboratory of Modern Optical Instrumentation, College of Information Science and Electronic Engineering, Zhejiang University, Hangzhou 310027, China. [2] ZJU-Hangzhou Global Science and Technology Innovation Center, Key Lab. of Advanced Micro/Nano Electronic Devices & Smart Systems of Zhejiang, Zhejiang University, Hangzhou 310027, China. [3] International Joint Innovation Center, ZJU-UIUC Institute, The Electromagnetics Academy, Zhejiang University, Haining 314400, China.

and crosstalk barriers blocking the further development of novel photonic systems, we focus on material active tuning [19] and source manipulation [11, 12, 20] in hyperbolic materials [21, 22].

In addition to the source manipulation, recent studies already show that the near field directional excitations obey Wigner's rule, which describes the spin (polarization) conservation in light-material interactions [23–26]. Since the source is engineered to the state with a certain polarization (spin), Wigner's rule implies that the possible exciton excited in solid can only be the polaritons that carry the same spin momentum as the light source [26]. Following this strategy, circularly polarized dipole, Huygens dipole, and Janus dipole are investigated to obtain different spin momentum matching, which lead to different directional excitations [23].

In this paper, we extend previously proposed scheme focusing on the control of the group velocity of hybrid plasmon-phonon polaritons in the graphene-*h*BN waveguide [27]. Instead of a single graphene-*h*BN waveguide, we renew our platform by a dual slab coupled waveguide which is symmetric with respect to the light source located at origin. As the graphene-*h*BN heterostructure supports hybrid polaritons, it extracts the momentum and energy information of evanescent waves from the dipole source. Since applied optical source is asymmetric along the direction of coupled dual symmetric waveguides, the upper heterostructure slab has a completely opposite behavior compared with the lower slab. Here, we report two different active tuning properties of directional excitation. On one hand, we show the reconfigurable directionality through the active tuning of material properties without changing the built-in optical source. The excitons fly toward one certain direction according to the sign of polariton's group velocities. Active tunability of group velocity is achieved with different graphene chemical potentials. To be specific, when graphene chemical potential is slightly doped $\mu_c = 0.1\,\mathrm{eV}$, graphene's conductivity is not strong enough to dominate hybrid polaritons, then the hybrid polaritons will behave as phonon polaritons. When graphene is heavily doped with $\mu_c = 0.4\,\mathrm{eV}$, graphene's conductivity becomes significant so that hybrid polaritons are evolving as plasmonic polaritons. On the other hand, we modify the integrated hybrid dipole to ensure the different directionalities, where diverse directional excitations are excited under circularly polarized dipoles, Huygens dipoles and Janus dipoles.

2. RESULTS AND DISCUSSION

The underlying physics are revealed by the dispersion relations of polarized supported by the graphene-*h*BN heterostructures [Figure 1]. Two *h*BN slabs are immersed in a silica substrate. Each *h*BN slab has a thickness of $d_{h\mathrm{BN}} = 15\,\mathrm{nm}$ and coated by two graphene sheets [Figure 1(a)]. Without loss of generality, such a structure is symmetric to the origin point where the hybrid dipole is placed. Electromagnetic model of such a platform is a simple 5-layer waveguide, as shown in Figure 1(b). Dual *h*BN slabs with hyperbolic dispersion and higher dielectric constant support the hybrid polaritonic modes. The uniaxial permittivity of *h*BN is retrieved from experimental results [28], i.e., $\overline{\overline{\epsilon}}_{h\mathrm{BN}} = \mathrm{diag}(\epsilon_{r,x}, \epsilon_{r,y}, \epsilon_{r,z})$, where $\epsilon_{r,x} = \epsilon_{r,y} \neq \epsilon_{r,z}$ are the components of relative permittivity parallel or perpendicular to the *h*BN plane (i.e., x-y plane), respectively. These *h*BN slabs are immersed in a silica substrate with the permittivity $\epsilon_{r,subs} = 3.455$; a proper gap distance is set to inhibit the coupling between dual *h*BN waveguides: $d_2 - d_3 = 230\,\mathrm{nm}$. Graphene sheets located at 4 *h*BN surfaces are described via the Random Phase Approximation (RPA) model [29]. An electron lifetime 0.1 ps and electron mobility $10{,}000\,\mathrm{cm^2V^{-1}s^{-1}}$ are set to extract the optical conductivity. Due to the recent advance in nanofabrication, the proposed structure in Figure 1 should be quite feasible in experiments.

Those supported hybrid plasmon-phonon polaritons are extracted from dispersion relations obtained in Figures 1(c)–(d). Gradually, we increase the graphene chemical potential from $\mu_c = 0.1\,\mathrm{eV}$ to $\mu_c = 0.4\,\mathrm{eV}$. Then the enlarged graphene plasmons will deeply modulate original *h*BN phonon polariton. The hybrid polaritons will be plasmon-like polaritons. For clarity, we define the sign of group velocity $v_g = d\omega/dk$ with respect to the sign of phase velocity $v_p = \omega/k$. If we set the phase velocity to be positive, i.e., $k > 0$, then a positive (negative) group velocity represents that the direction of the group velocity is identical(opposite) to that of the phase velocity. Or if the phase velocity is negative, i.e., $k < 0$, then a "positive"("negative") group velocity means that the sign of group velocity is negative("positive"), directing $-x(+x)$. As Figures 1(c)–(d) illustrate, at frequency 24.3 THz, when graphene sheets are slightly doped $\mu_c = 0.1\,\mathrm{eV}$ [Figure 1(c)], the hybrid graphene-*h*BN

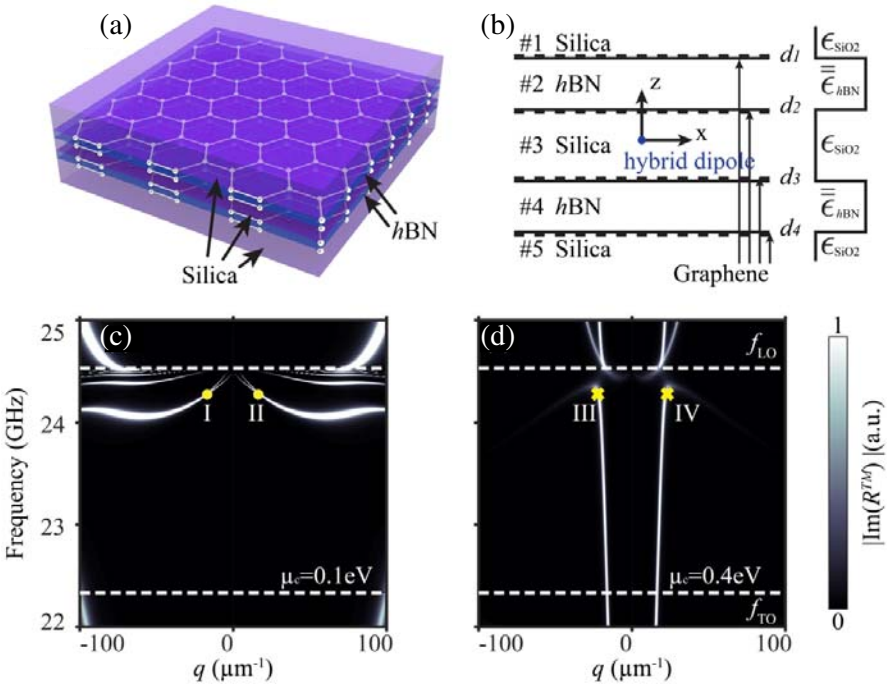

Figure 1. Hybrid plasmon-phonon polaritons in graphene-hBN multilayer heterostructures. (a) Structural schematic of two weak coupled hBN (blue block) immersed in a silica background (purple block). Their boundaries are covered by monolayer graphene sheets. (b) Electromagnetic model of the 5-layer waveguide structure. Without loss of generality, the coupled waveguides are symmetric according to the hybrid electric/magnetic dipoles located at the origin; both hBN slabs are 15 nm thick and separated by a 100 nm-thick silica gap; each dashed lines on the boundaries of hBN slabs represents a monolayer graphene monolayer. (c)–(d) Dispersion relation of hybrid plasmon-phonon polaritons in the 5-layer waveguide. The chemical potential μ_c of graphene is different, namely. $\mu_c = 0.1\,\text{eV}$ in (c), $\mu_c = 0.4\,\text{eV}$ in (d). A false-color plot of reflection coefficient $|\text{Im}(R^{\text{TM}})|$, which can be used to visualize the polaritonic dispersion. Those singularity poles (bright lines, spots) of R imply the polaritonic modes supported in the 5-layer waveguide. The dashed lines correspond to the transverse optical (TO) and longitudinal optical (LO) frequencies of the first reststrahlen band, respectively.

polaritons perform similar to hBN phonon polaritons. The negative group velocities mean that the sign of group velocities and phase velocities are opposite: when phase velocity is negative(positive), i.e., $k < 0 (k > 0)$, then the group velocity is positive(negative), corresponding to polaritons I(II). By increasing the graphene chemical potential to $\mu_c = 0.4\,\text{eV}$ (Figure 1(d)), graphene plasmons will dominate the hybrid polaritons. Then the sign of group velocities is identical to the sign of phase velocities, corresponding to polaritons III(IV).

To visualize the directional excitation, spatial distributions of electromagnetic fields in the 5-layer heterostructure waveguide are investigated for all dipolar sources. At the plane of interest (x-y plane), we start from TM modes, whose primary fields are calculated as follows:

$$E_{z,j} = \int_{-\infty}^{\infty} dk_\rho \left(ik_\rho^2 H_0\left(k_\rho\rho\right) p_x - \frac{k_\rho^3}{k_{z,3}} H_1\left(k_\rho\rho\right) p_z + \frac{k_\rho^3}{k_{z,3}} m_y H_0\left(k_\rho\rho\right) \right) A_j \left(\pm e^{ik_{z,j}|z|} \mp \tilde{R}_{j,j\pm1} e^{-ik_{z,j}(z+2d_j)} \right)$$

The subscript j in all terms is defined with respect to different waveguide regions shown in Figure 1(b), and regions of the substrate silica are denoted as $j = 1, 3, 5$, and regions of hBN waveguide are labeled as $j = 2, 4$. The "+"("−") sign in Equation (1) is adopted when $z > 0$ ($z < 0$). k_ρ and

$k_{z,j} = \sqrt{k_0^2 \frac{\epsilon_{r,x,j}}{\epsilon_{r,z,j}} - k_\rho^2}$ are the components of the wavevectors parallel and perpendicular to the interface, respectively. Amplitude coefficients A_j can be derived from boundary conditions at all 4 boundaries, and the generalized reflection coefficients $\tilde{R}_{j,j\pm1}$ can also be obtained analytically from the boundaries; $H_0(H_1)$ is the first kind Hankel function of zeroth(first) order.

Since the integral has multiple singularities on the integration path, they should be treated carefully to obtain a meaningful result without violating the physics [30]. A Sommerfeld path integral is performed here (see Figure 2). All singularities can be divided into two types. One type is the intrinsic poles introduced by materials, which are located at the points $k = k_j = \frac{\omega}{c}\sqrt{\epsilon_{r,x,j}}$. The other is polaritonic poles supported in the waveguide system. According to Cauchy's theorem, the enclosed Sommerfeld path integrates the entire top Riemann sheet. Thus, the field calculated only consists of the information of intrinsic poles and polaritonic poles. In passive regimes, the intrinsic poles are located in the top Riemann sheet, such that the Sommerfeld path should take a detour to include the contribution of them. While polaritonic pole with positive(negative) group velocity lies in the top(bottom) Riemann sheet, Sommerfeld path is chosen to include (exclude) the pole contributions.

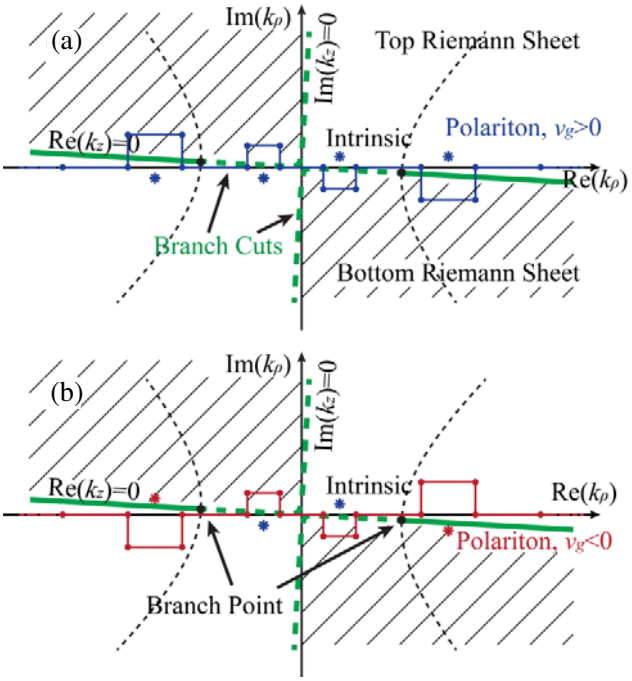

Figure 2. Sommerfeld integration path (blue and red lines) used in the numerical calculation of the distribution of fields excited by the dipoles. The excited polaritons with (a) positive/(b) negative group velocity with respect to the phase velocity should be dealt with different Sommerfeld integration paths. The Sommerfeld integration path is considered in the real frequency domain and in the complex k_ρ domain. The branches and corresponding Riemann sheets of k_z are derived from k_ρ. The shaded regions are bottom Riemann sheet of k_z while the blank regions are top Riemann sheet. They are addressed with respect to the hyperbolic coordinate of k_z. Divided by branch points, the coordinate of k_z are separated as branch cuts (green dashed lines implying real axis, $\mathrm{Im}(k_z) = 0$) as well as the imaginary axis (green solid lines referring imaginary axis $\mathrm{Re}(k_z) = 0$).

First, we consider a Circular dipole whose dipole moments are $\mathbf{p} = (p_x, 0, p_z)$, where $p_x = 1, p_z = i$. Electric dipoles along x and z directions have a phase difference of $\frac{\pi}{2}$. The circularly polarized dipole excites one-way hybrid plasmon phonon polaritons. From the excitation intensity obtained in Figure 3(a), it is clear that Circular dipole only carries the evanescent quasi-particle at a unique direction, which determines the helicity of excited one-way polaritons in graphene-hBN slabs. Meanwhile, the graphene-hBN slab on top of the circular polarized dipole source is antisymmetric to

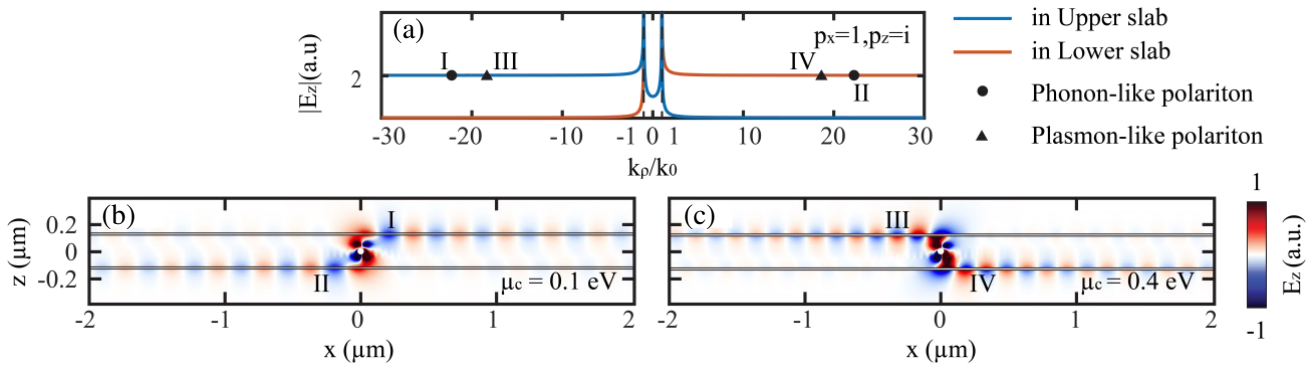

Figure 3. Field distributions of excited polaritons in the proposed 5-layer waveguide subject to a circularly polarized electric dipole at 24.3 THz. The electric dipole is defined as $\bar{p} = (p_x, 0, p_z)$, $\bar{m} = (0, 0, 0)$, where $p_x = 1$ and $p_z = i$. The graphene sheets are doped with chemical potential μ_c. (a) Magnitude of the evanescent quasi-particles carried by the circularly polarized dipole. In upper(lower) slab, the evanescent wave are mostly corresponded to negative(positive) wavevector, *viz.* negative(positive) sign of phase velocity. (b) Excited phonon-like polaritons (I, II) with the opposite sign between group velocity and phase velocity. (c) Excited plasmon-like polaritons (III, IV) with the identical sign between group velocity and phase velocity.

the lower graphene-*h*BN slab with respect to the position where dipole source is located (origin). Then, the helicity of Circular dipole is flipped in the upper slab with respect to the lower one. Therefore, the supported polaritons' helicity and directionality shall follow. In other words, the directionality in the upper slab shall be aligned to the other side. As shown in Figure 3(b), when graphene chemical potentials are low, i.e., $\mu_c = 0.1\,\text{eV}$, the excited phonon-like polaritons have negative group velocities. In the upper graphene-*h*BN slab, the polariton has a phase velocity $v_p < 0$ and a group velocity $v_g > 0$. Its energy goes in $+x$ direction while its phase propagates in $-x$ direction (phonon-like polariton mode "I"). In the lower waveguide, the polariton has a positive phase velocity and negative group velocity, $v_p > 0$ and $v_g < 0$, then the polariton goes to $-x$ with a reversed phase direction goes to $+x$ (phonon-like polariton mode "II"). Similarly, as the heavily doped graphene ($\mu_c = 0.4\,\text{eV}$) tailors the hybrid polaritons from phonon-like to plasmon-like, the signs of group velocities of hybrid polaritons are tuned to be identical with phase velocities, which will flip the propagation directions in both graphene-*h*BN slabs (see Figure 3(c)). The plasmon-like polariton travels to $-x$ direction in the upper graphene-*h*BN slab (plasmon-like polariton mode "III") while goes in $+x$ direction in the lower one (plasmon-like polariton mode "IV").

It is worth mentioning that the group velocity indicates the transportation of energy flow. In a causal system, the energy flow can only come from the source $x = 0$ and forward to the far field. As the spin momentum locks the wavevector to be positive ($k > 0$) in lower slab and negative ($k < 0$) in upper slab, the sign of phase velocities follows as $v_p = \omega/k$, so that the phase in upper(lower) slab can only propagate towards $-x(+x)$ direction. In case the sign of group velocities is identical(opposite) to the sign of phase velocities under heavily(lightly) doping, in the upper graphene-*h*BN slab, the excited polaritons can only go away from the source towards left(right) while in the lower graphene-*h*BN slab, the excited polaritons can only flee to the right(left).

As the circularly polarized dipole has been intensively studied, here we extend a similar phenomenon to another source type, the Huygens dipole. A Huygens dipole has a dipole moment of $\mathbf{p} = (0, 0, p_z)$, $\mathbf{m} = (0, m_y, 0)$ where $p_z = i$ and $m_y = i20c$, electric dipole and magnetic dipole do not have any phase differences. Here, Kerker condition governs the magnitude of electric and magnetic dipoles, which reads $p = m/c$. Other than a Circular dipole, Huygens dipole is symmetric with respect to the z direction. The upper graphene-*h*BN slab behaves exactly the same as the lower graphene-*h*BN slab. As Figure 4(a) demonstrates, the evanescent fields carried by the Huygens dipole are degenerated among all momentums. Both phonon-like and plasmon-like polaritons can only be excited at the $+x$ direction carrying the same momentum. Phase velocities in both waveguides are locked to be positive:

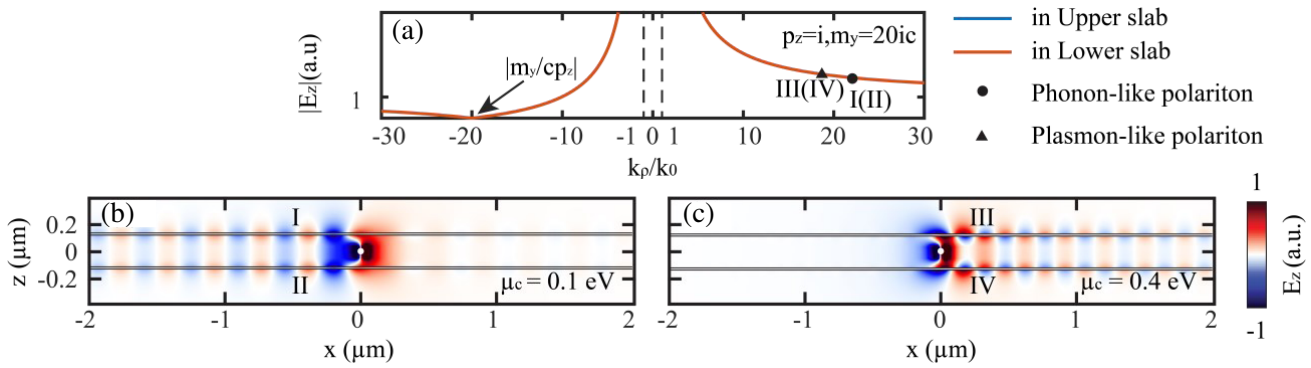

Figure 4. Field distributions of excited polaritons in the proposed 5-layer waveguide subject to a Huygens dipole at 24.3 THz. The Huygens dipole has $\bar{p} = (0, 0, p_z)$ and $\bar{m}/c = (0, m_y, 0)$, where $p_z = i$ and $m_y/c = 20i$. The graphene sheets are doped with a chemical potential of μ_c. (a) Magnitude of the evanescent field carried by the Huygens dipole, the evanescent quasi-particles are highly suppressed to the negative wavevector region, the quasi-particle will vanish at a certain wavevector $\frac{k_\rho}{k_0} = \frac{m_y}{cp_z} = 20$. (b) Excited phonon-like polaritons (I, II) with the opposite sign between group velocity and phase velocity. (c) Excited plasmon-like polaritons (III, IV) with the same sign between group velocity and phase velocity.

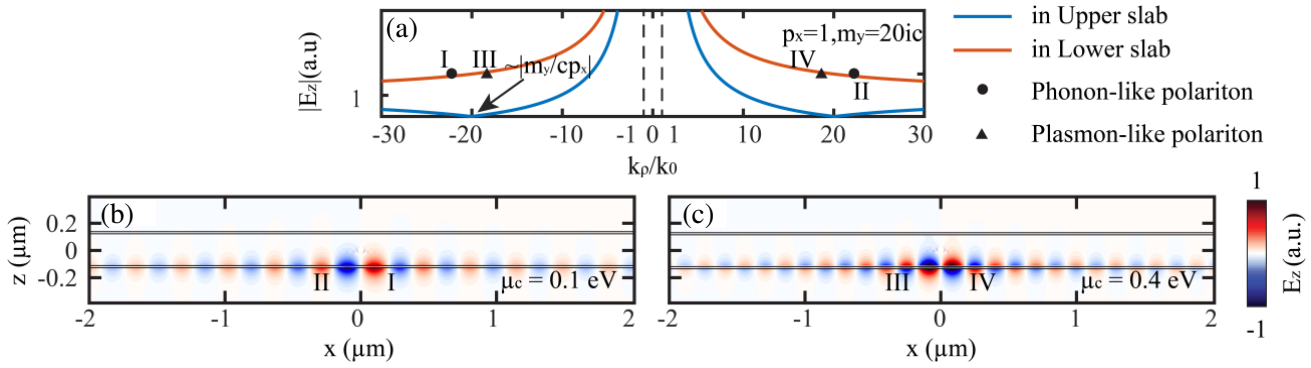

Figure 5. Field distributions of excited polaritons in the proposed 5-layer waveguide subject to a Janus dipole at 24.3 THz. The Janus dipole has dipole moment $\bar{p} = (1, 0, 0)$ and $\bar{m}/c = (0, 20i, 0)$, where $p_x = 1$ and $m_y/c = 20i$. The graphene sheets are doped with a chemical potential of μ_c. (a) Magnitude of the evanescent field carried by the Janus dipole, the evanescent quasi-particles in the upper slab are highly suppressed. The quasi-particle will vanish at a certain wavevector $\frac{k_\rho}{k_0} \approx \left|\frac{m_y}{cp_x}\right| = 20$. (b) Excited phonon-like polaritons (I, II) with the opposite sign between group velocity and phase velocity. (c) Excited plasmon-like polaritons (III, IV) with the same sign between group velocity and phase velocity.

the phase propagates along $+x$. In this manner, when graphene pairs are slightly doped ($\mu_c = 0.1\,\text{eV}$), the phonon-like polaritons (I, II) with negative group velocities invert the transport energy in both slabs toward $-x$ (Figure 4(b)). While both graphene pairs are heavily doped ($\mu_c = 0.4\,\text{eV}$), the plasmon-like polaritons (III, IV) are directed to the $+x$ (Figure 4(c)).

For Janus dipole, the stories are quite different. As Figure 5(a) shows, a Janus dipole of dipole moments $\mathbf{p} = (1, 0, 0)$, $\mathbf{m} = (0, i20c, 0)$ is a surprisingly symmetric source all over the momentum spaces. The asymmetry only exists between different waveguides. Polaritonic excitations through evanescent quasi-particles are highly suppressed in the upper waveguide while being excitable in the lower waveguide. If graphene chemical potential is low, phonon-like polariton in the lower slab has a positive(negative) group velocity, and a negative(positive) group velocity will be excited on the right(left)

side. The energy goes to $\pm x$ direction while the phases velocities point the source (see Figure 5(b), polariton mode I(II)). If graphene chemical potential is high, plasmon-like polariton in lower slab is excited with identical sign of group and phase velocities. The field is going away from the Janus dipole on both sides (see Figure 5(c), polariton mode III and IV).

It should be noted that the gap distance between graphene-hBN slabs is carefully designed because the proposed 5-layer graphene coated hBN dual-slab waveguide should be a weak coupled waveguide. Despite the mixture of graphene plasmon polaritons and hBN phonon polaritons in each individual waveguide, the interference between two graphene-hBN slabs is cruel. When both graphene-hBN slabs are not well placed with a silica gap of proper thickness, the interference may result in some unexpected phenomena. For example when the silica gap is too thin, the guiding mode will split into 2 separate wavevectors — the even mode and odd mode — single mode waveguide is no longer fulfilled, which will severely limit the application in optical devices; if the gap is moderate, one-way propagation may be unpredictable in case two waveguides may build a directional coupler which guides the field from one slab to another; if the gap is too thick, it is difficult to couple the energy efficiently from the dipole source to the hybrid plasmon-phonon polaritons since the evanescent waves decay exponentially. A 230 nm silica gap is judiciously chosen for all considerations listed here. Tuning the silica gap allows us to further investigate the potentials of the proposed multilayer graphene-hBN heterostructures waveguide.

3. CONCLUSION

In summary, we have provided two different schemes for active manipulation on tunable directionalities in a 5-layer waveguide composed of two graphene encapsulated hBN slabs. We reveal the different spin locking properties between Circular dipole and Huygens dipole. Circular dipole is antisymmetric to the origin; Huygens dipole is symmetric vertically; and Janus dipole is symmetric horizontally. Such diversity provides a further flexibility in controlling the direction of excitons. Both Circular and Huygens dipoles support hybrid plasmon-phonon polaritons. Unusual backward transportation of polaritons is exhibited when graphene chemical potentials are low, and hBN phonon polaritons are dominant; graphene plasmon polaritons control the waveguide when graphene chemical potential is high. Those polaritons with different group velocities extract the single direction coupling information of evanescent quasi-particles from dipole sources. Such a platform shall lead to more interesting phenomena in selective coupling and quasi-particle behaviors, as well as the underlying physics of photon momentum and energy.

ACKNOWLEDGMENT

The work at Zhejiang University was sponsored by the National Natural Science Foundation of China (NNSFC) under Grants No. 61625502, No. 11961141010, and No. 61975176, the Top-Notch Young Talents Program of China, the Fundamental Research Funds for the Central Universities (2021FZZX001-19), and Zhejiang University Education Foundation Global Partnership Fund.

REFERENCES

1. Ma, W., et al., "In-plane anisotropic and ultra-low-loss polaritons in a natural van der Waals crystal," *Nature*, Vol. 562, 557, 2018.
2. Chervy, T., et al., "Room temperature chiral coupling of valley excitons with spin-momentum locked surface plasmons," *ACS Photonics*, Vol. 5, 1287, 2018.
3. Gururanayanan, S., et al., "Electrically driven unidirectional optical nanoantennas," *Nano Letters*, Vol. 17, 7433, 2017.
4. Divinskiy, B., et al., "Excitation and amplification of spin waves by spin-orbit torque," *Advanced Materials*, Vol. 30, 1802837, 2018.
5. Sinev, I., et al., "Chirality driven by magnetic dipole response for demultiplexing of surface waves," *Laser & Photonics Reviews*, Vol. 11, 1700168, 2017.
6. Wang, M., et al., "Magnetic spin-orbit interaction of light," *Light: Science & Applications*, Vol. 7, 24, 2018.

7. Li, P., et al., "Optical nanoimaging of hyperbolic surface polaritons at the edges of van der Waals materials," *Nano Letters*, Vol. 17, 228, 2017.
8. Li, Y., et al., "Orientation-dependent exciton-plasmon coupling in embedded organic/metal nanowire heterostructures," *ACS Nano*, Vol. 11, 10106, 2017.
9. Sinev, I., et al., "Steering of guided light with dielectric nanoantennas," *ACS Photonics*, Vol. 7, 680, 2020.
10. Liu, F., et al., "Surface-plasmon-polariton diode by asymmetric plano-concave nanocavities," *Advanced Optical Materials*, Vol. 6, 1701226, 2018.
11. Cao, S., et al., "Directional light beams by design from electrically driven elliptical slit antennas," *Beilstein Journal of Nanotechnology*, Vol. 9, 2361, 2018.
12. Stauber, T., et al., "Unidirectional plasmonic edge modes on general two-dimensional materials," *2D Materials*, Vol. 6, 045023, 2019.
13. Atabaki, A., et al., "Integrating photonics with silicon nanoelectronics for the next generation of systems on a chip," *Nature*, Vol. 556, 349, 2018.
14. Miri, M., et al., "Exceptional points in optics and photonics," *Science*, Vol. 363, 42, 2019.
15. Cheben, P., et al., "Subwavelength integrated photonics," *Nature*, Vol. 560, 565, 2018.
16. Sengupta, K., et al., "Terahertz integrated electronic and hybrid electronic-photonic systems," *Nature Electronics*, Vol. 1, 622, 2018.
17. West, P., et al., "Searching for better plasmonic materials," *Laser & Photonics Reviews*, Vol. 4, 795, 2010.
18. Ni, G., et al., "Fundamental limits to graphene plasmonics," *Nature*, Vol. 557, 530, 2018.
19. Gangaraj, S., et al., "Unidirectional and diffractionless surface plasmon polaritons on three-dimensional nonreciprocal plasmonic platforms," *Physical Review B*, Vol. 99, 245414, 2019.
20. Picardi, M., et al., "Experimental demonstration of linear and spinning Janus dipoles for polarisation- and wavelength-selective near-field coupling," *Light: Science & Applications*, Vol. 8, 52, 2019.
21. Kapitanova, P., et al., "Photonic spin Hall effect in hyperbolic metamaterials for polarization-controlled routing of subwavelength modes," *Nature Communications*, Vol. 5, 3226, 2014.
22. Ferrari, L., et al., "Hyperbolic metamaterials for dispersion-assisted directional light emission," *Nanoscale*, Vol. 9, 9034, 2017.
23. Yermakov, O., et al., "Spin control of light with hyperbolic metasurfaces," *Physical Review B*, Vol. 94, 075446, 2016.
24. Picardi, M., et al., "Janus and Huygens dipoles: Near-field directionality beyond spin-momentum locking," *Physical Review Letters*, Vol. 120, 117402, 2018.
25. Zhong, Y., et al., "Toggling near-field directionality via polarization control of surface waves," *Laser & Photonics Reviews*, Vol. 15, 2000388, 2021.
26. Wigner, E., et al., "Ueber die Erhaltungssätze in der Quantenmechanik," *Mathematisch-Physikalische Klasse*, Vol. IIa, 375, 1927.
27. Jiang, Y., et al., "Group-velocity-controlled and gate-tunable directional excitation of Polaritons in graphene-boron nitride heterostructures," *Laser & Photonics Reviews*, Vol. 12, 1800049, 2018.
28. Woessner, A., et al., "Highly confined low-loss plasmons in graphene-boron nitride heterostructures," *Nature Materials*, Vol. 14, 421, 2015.
29. Shuang, K., et al., "Dielectric function and plasmon structure of stage-1 intercalated graphite," *Physical Review B*, Vol. 34, 979, 1986.
30. Chew, W., *Waves and Fields in Inhomogeneous Media*, Ch. 2, Wiley-IEEE Press, 1995.